Chemical and Process Engineering: New Frontiers, 2023, 44(3), e25
DOI: 10.24425/cpe.2023.146727

Flow modification of non-woven oil-mist filters with MTMS-based aerogel structure

Bartosz Nowak[1*], Marta Bonora[2], Agnieszka Hahaj[1], Jakub M. Gac[1]

[1] Warsaw University of Technology, Faculty of Chemical and Process Engineering, Waryńskiego 1, 00-645 Warsaw, Poland
[2] GVS Filter Technology, Via Roma 5040069, Zola Predosa (Bologna), Italy

*** Corresponding author:**
e-mail:
bartosz.nowak@pw.edu.pl

Article info:
Received: 4 April 2023
Revised: 20 June 2023
Accepted: 26 June 2023

Abstract
A significant challenge of modern technology is the design of high-efficiency filters that allow more effective removal of aerosol particles suspended in the air, e.g. micron and submicron oil droplets. Our previous work has proven that aerogel structure deposition on fibre surface is a promising method for post-production improvement of the oil-mist filter performance. In this work, a modification of the previously described method was proposed, consisting in carrying out the process in the flow (semi-batch) regime, i.e. the streams of reagents successively pass through the filter in a self-designed and self-made modification chamber. The effect of the reactant flow rate and the order of reactants (precursor/catalyst or catalyst/precursor solutions) on the mass of deposited aerogel, and thus – also on the filtration efficiency during the removal of oil mist droplets and the pressure drop accompanying the airflow – is presented and described. The possible routes of modification scaling-up are discussed with defined unit operations.

Keywords
oil mist filtration; filter modification; flow-system; sol-gel technique; MTMS aerogel

1. INTRODUCTION

Oil mists are generated by many industrial processes, including engine crankcase ventilation, cutting operations and the generation of compressed air by oil-lubricated compressors. Removing these mists to avoid further downstream problems or meet health and safety regulations is necessary. Filtration utilising fibrous (non-woven) materials is one of the most common techniques employed in oil-mist separation. Mist droplets are collected on the fibres due to diffusion, interception or inertial impaction mechanisms (Brown, 1993). With an increasing amount of droplets being captured by fibre, they tend to coalesce into larger drops (Yarin et al., 2006). Gravity and flow forces determine their transport within the filter (Starnoni and Manes, 2022). If the fibre is very well wetted by the droplet-forming liquid, these droplets eventually spread on the fibre and form a liquid film (Agranovski and Braddock, 1998). Such films and coalesced drops can join together and form liquid bridges at fibre intersections and between fibres (Liew and Conder, 1985; Mullins et al., 2004), which under capillary forces remain equalised.

Improving filter operating performance – the efficiency of oil droplet separation, its retention and dripping, as well as the generated flow resistance – is an aspect of interest to engineers. The structural parameters of the filter material, such as packing density and fibre mean diameter (and, following that, its surface mass), affect the development of the collector (i.e. fibres in the case of fibrous filters) surface (Charvet et al., 2010; Jackiewicz and Werner, 2015). This, in turn, translates into the separation efficiency of oil droplets in a wide range of fractions, as well as the pressure drop of the material in a dry state (initial conditions) (Gac, 2015; Sun and Chen, 2002). According to the behavioural model of oil aerosol filtration dynamics, which has been dominant in recent years (Kampa et al., 2014; Kampa et al., 2015), the key aspect influencing the transport of oil inside the filtration structure is the wettability of the material (Kolb et al., 2018; Penner et al., 2021; Xu et al., 2021). Hence a modification, which simultaneously alters the material wettability and increases collector surface area is highly desired.

Sol–gel science and technology offer the possibility of modifying the properties and combine functionalities in a single material (Mekonnen et al., 2021). One of the most significant benefits of the sol–gel technology is the use of low-temperature conditions and insensitivity to the surrounding atmosphere, allowing its utilisation with various materials, including textile substrates, which cannot tolerate high temperatures (Ismail, 2016). Silica aerogel-fibre composites can be obtained via various processes, leading to different forms (Mazrouei-Sebdani et al., 2022). Fibres can be mixed with primary sol to achieve higher mechanical properties of received fibre-reinforced aerogel (Haq et al., 2017) or aerogel-fibre fleece when passed through a spinning nozzle (Tepekiran et al., 2019; Wu et al., 2013). Aerogel-filled fibres can be extruded from the mixture of polymer with previously synthesized aerogel granules (Joung et al., 2018). However, the above listed processes focus on the improvement of mechanical and thermal properties and cannot be used to meet air purification requirements. An alternative way is to impregnate the fibrous mat with a sol (Kim et al., 2008; Linhares et al., 2019, typically via dip-coating (Ortelli et al., 2015), spray-

coating (Shams-Ghahfarokhi et al., 2019) or spin-coating (Azani et al., 2019).

As exploited in previous works (Nowak et al., 2017), a combination of sol-gel synthesis with the melt-blown fabrication of fibrous materials can overcome low separation efficiency and coalesced oil drift towards the filter rear side, via increasing an effective collector area and oil retention, thanks to an addition of oleophilic porous structure in filter volume (Nowak et al., 2022a; Nowak et al., 2022b). Fibrous filter modification with an aerogel structure is based on material immersion into the condensing sol. Thanks to the adjustment of solution composition and gel volume shrinkage, assisting ambient pressure drying (APD) method, the aerogel structure deposition takes place only on the fibre surface and not in the non-woven pores (space between fibres). Such a combination of macro- and mesopores results in higher filtration efficiency without causing a significant rise in pressure drop (Kim et al., 2016; Mosanenzadeh et al., 2020).

This article describes an attempt to transfer filter modification from the batch method of immersion in a reacting mixture to the flow/semi-batch process. The work aimed at maintaining the previously developed sol-gel synthesis procedure, so it is based on gel condensation on material fibres, to obtain deposits in the form of a porous structure, and not on the adsorption of the sol, which would form a continuous layer. The modification system and procedure proposed in the paper may be treated as a semi-step before scaling up.

2. MATERIALS AND METHODS

2.1. Native filter characterisation

Polypropylene (PP) non-woven filters were manufactured on a semi-industrial machine in the Faculty of Chemical and Process Engineering WUT, using melt-blown technology (Jackiewicz and Werner, 2015). The mean fibre diameter was determined with scanning electron microscope (SEM, Hitachi TM-1000) images. The wettability of fibres by water and oil was measured utilizing the sessile droplet method (Dataphysics OCA 25 Goniometer) and described previously (Nowak et al., 2021; Nowak et al., 2022b). The filter characteristics are summed up in Table 1. Before modification, the filter exhibited hydrophobic and moderate-oleophilic characteristics.

Table 1. Characteristics of native polypropylene filter.

Arithmetic mean fibre diameter [μm]	6.41 (±4.18)
Filter average thickness [mm]	2.86 (±0.03)
Packing density [%]	8.11 (±0.02)
Number of layers [–]	25.00
Surface weight [mg/cm^2]	21.01 (±0.27)
Filter mass [g]	3.72 (±0.05)
Water/air contact angle [°]	152.04 (±4.35)
Oil/air initial contact angle [°]	87.32 (±3.05)

2.2. Filter modification

The flow modification was tested in different configurations, utilising a one-step base sol-gel method and a two-step acid-base sol-gel method. In each case, the modification was divided into two stages in which a different solution was passed through the material.

For the configuration based on the one-step synthesis, the reaction solution consisted of methyltrimetoxysilane (MTMS, Sigma–Aldrich), methanol (Stanlab) and concentrated ammonium hydroxide (25%, Eurochem GBD), which catalysed the hydrolysis and condensation reactions. In the case of a two-step synthesis, one of the solutions was a hydrolysed (for 1 hour) precursor – MTMS with methanol and 0.01M aqueous oxalic acid (Sigma–Aldrich) – and the second solution, which was the condensation catalyst (base) – ammonium hydroxide (1M). Both solutions that were used to modify the round filter, 15 cm in diameter, are summed up in Table 2. For each precursor/base configuration, the influence of flow rate was investigated. The flow rates equalled 0.92, 1.62, 2.32, 3.02 and 3.72 mL/s (which corresponded to pump adjustment from 10 to 50 rpm in a 10 rpm step). For a chosen flow rate, additional modifications were performed, with the inverse stage – marked as base/precursor.

The modification procedure followed several steps. The fibrous filter pre-wetted in isopropanol was placed inside a modifying cell (modification setup shown in Fig. 1). To prevent any leakage, the cell was fixed with screws. The stage 1 solution was fed from reservoirs (1) using a peristaltic pump (2) at a pre-set flow rate. As soon as the stage 1 tank was emptied, a three-way valve was turned on and the stage 2 solution was dispensed. After passing through the modifying cell (3), the solutions were collected in a beaker (4). The time of immersion of the filter in individual solutions was dependent on flow rate and the volume of solutions and ranged from 10.75 s (in the base solution at the flow rate of 3.72 mL/s) to 163 s (in the precursor solution at two-step modification and the flow rate of 0.92 mL/s). After both solutions from both stages passed through the cell, the modified filter was slowly dried in the oven at 50°C at ambient pressure (APD), which usually took no more than 5 hours.

The flow system modification was carried out using a self-made (CNC machine tool, VMC 650, Avia S.A.) PP cell (photo shown in Fig. 1B) The modification chamber was designed to ensure even horizontal distribution of the modifying solution. The inlet to the cell was placed tangent to the outer wall. A concentric converging channel distributed the solutions evenly below the filter. After filling up the channel, the solution passed upwards, through the non-woven material and leaft the modifying cell through the outlet centrally located in the lid.

Table 2. The modification configurations.

Configuration	1st stage solution	2nd stage solution
1-step (precursor/base)	10 mL MTMS – 100 mL MeOH	40 mL NH_4OH (25%)
1-step (base/precursor)	40 mL NH_4OH (25%)	10 mL MTMS – 100 mL MeOH
2-step (precursor/base)	10 mL MTMS – 100 mL MeOH – 40 mL $C_2H_2O_4$ (0.01M)	40 mL NH_4OH (1M)
2-step (base/precursor)	40 mL NH_4OH (1M)	10 mL MTMS – 100 mL MeOH – 40 mL $C_2H_2O_4$ (0.01M)

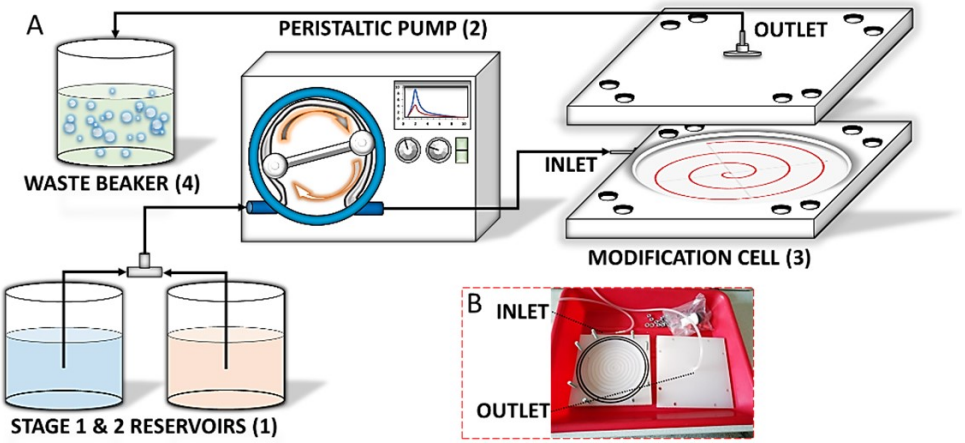

Figure 1. (A) Flow-modification setup scheme and (B) disassembled modification cell photo with a visible concentric channel in the bottom part.

All filters were weighed before and after the modification procedure to determine the amount of deposited aerogel and packing density (according to Equation (1)):

$$\alpha = \frac{\frac{m_{PP}}{\rho_{PP}} + \frac{m_{ag}}{\rho_{sk}}}{V} \quad (1)$$

where: α – packing density, m_{PP} – mass of polypropylene filter, ρ_{PP} – polypropylene density, m_{ag} – the mass of deposited aerogel, ρ_{sk} – MTMS skeletal density, V – material volume (the filter was cut to fit the chamber).

PP filters and MTMS-based aerogel skeletal density were measured on a helium pycnometer (Humi–Pyc Model 2) and equal 0.906 g/cm^3 and 1.205 g/cm^3, respectively.

After modification, the surface foil layer, which formed at the filter surface as an effect of surface tension and increased solvent evaporation (Nowak et al., 2022b), was removed from the top of the modified fibrous material and filters (marked as without the foil layer) were weighted again. Materials were characterised via a scanning electron microscope. Samples were first sputtered with a conductive gold/palladium nanolayer for better image resolution.

To estimate the oil sorption capacity of modified filters, five samples (4 cm in diameter) with known weight were placed in bis(2-ethylhexyl) sebacate (Sigma–Aldrich) oil for 24 hours. The adsorption capacity was calculated, as a mass of liquid per material area, from the following equation (2):

$$\text{adsorption capacity} = \frac{\text{mass}_{wet} - \text{mass}_{dry}}{\text{material area}} \left[\frac{g_{oil}}{cm^2}\right] \quad (2)$$

2.3. Investigation of filtration properties

The separation efficiency tests of non-woven filters and the pressure drop on the fibrous material were carried out using an HFP 2000 filter testing system (PALAS GmbH). A scheme of this setup is shown in Fig. 2A. The main elements of this setup are the horizontal channel (length – 1 m, diameter – 15 cm) followed by the adapter enabling the insertion of a 177 cm^2 flat filter (oriented vertically, in the form of a circle with a diameter of 15 cm).

The PLG 2000 liquid spray generator (Particle Liquid Generator) can disperse aerosol with a known and constant droplet diameter distribution (Fig. 2B). Bis (2-ethylhexyl) sebacate oil (DEHS, Sigma–Aldrich) was used in the experiments. This fluid is recommended by PN-EN ISO 16890-1:2017-01E for mist filtration studies owing to high durability of the obtained droplets (resulting from long evaporation time). The spectrometric particle counter Welas 1200, enabling the registration of drops with a diameter of 0.19–10.00 µm was utilised to determine the droplet size distribution. The mass concentration of DEHS aerosol was equal to 40 g/h. The separation

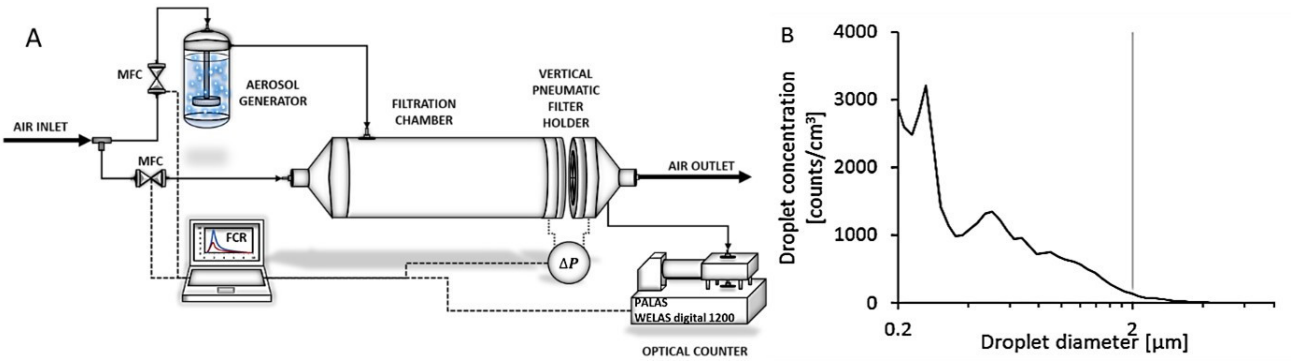

Figure 2. (A) Scheme of HFP 2000 filter testing system. (B) Generated droplet size distribution.

efficiency and pressure drop across the filter ΔP (measuring points before and after filter insert, as shown in Fig. 2A) were calculated concerning the results obtained with an empty container, i.e., without a filter sample. The test parameters are listed in Table 3.

Table 3. The filtration test parameters.

Investigated droplet size range d_P [µm]	0.19–8.00
DEHS density ρ_P [g/cm^3]	0.91
Gas face velocity u_0 [m/s]	0.20

3. RESULTS

3.1. Influence of reagent flow rate

To better understand the presented results, one must first familiarize oneself with the characteristics of both sol-gel methods and discuss their differences. The one-step sol-gel method of aerogel synthesis consists of precursor molecule hydrolysis and the following condensation reaction, which results in solid skeleton formation. The pH value is decisive for the relative rates of hydrolysis and condensation of alkoxysilanes (Fig. 3). In acidic conditions, hydrolysis is favourable, while condensation is the rate-determining step. A great number of hydrolysed precursor monomers or small oligomers, reach with reactive Si-OH groups, are present in the solution (Hüsing and Shubert, 1998). The opposite situation is observed in neutral-to-alkaline conditions, where hydrolysis is the rate-determining step. In this pH range, condensation occurs on the central silicon atom of the oligomer unit, resulting in a "colloid-like" gel structure with a large secondary particle diameter. At a pH value of approximately 11.7 (Dong et al., 2005), the hydrolysis reaction is again the favourable one, resulting in condensation at the terminal silicon atom, leading to a small-pore, "polymer-like" gel network formation.

The sol-gel method, which utilizes the favourable reaction pH, was first introduced by Brinker et al. (1982). The hydrolysis reaction occurs in the presence of an acidic catalyst, followed by a pH shift by adding a basic catalyst aqueous solution, which starts the condensation reaction. In the case of the presented MTMS-based synthesis, the condensation in an acid environment is negligible as it takes hours, while hydrolysis is measured in minutes. The condensation reaction in a two-step sol-gel method is less sensitive to pH changes. However, it is worth noticing that pH also affects it, by changing the reaction kinetics (Borzęcka et al., 2023) and, along with solution composition (Borzęcka et al., 2020), gel morphology.

The reagent flow rate influence on the amount of MTMS-based aerogel deposited on the PP filter is shown in Fig. 4A. An increasing flow rate decreases aerogel mass, which can be explained by precursor solution removal from the material volume. Fig. 4B shows that the deposited amount of aerogel does not affect the oil sorption capacity. A low amount of fibre aerogel does not increase oil sorption, as most of the

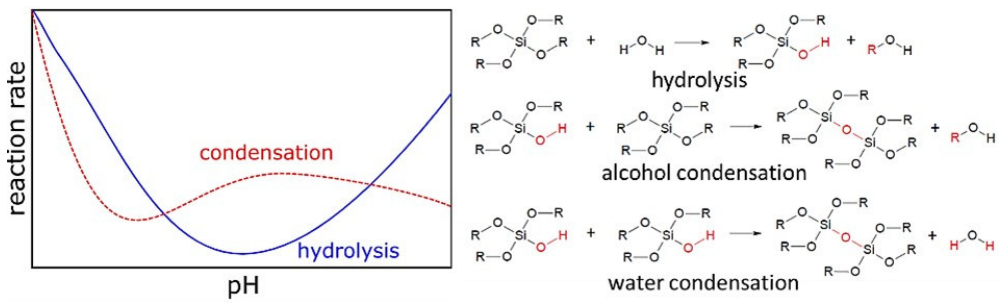

Figure 3. Influence of pH on reaction rate (Hüsing and Shubert, 1998).

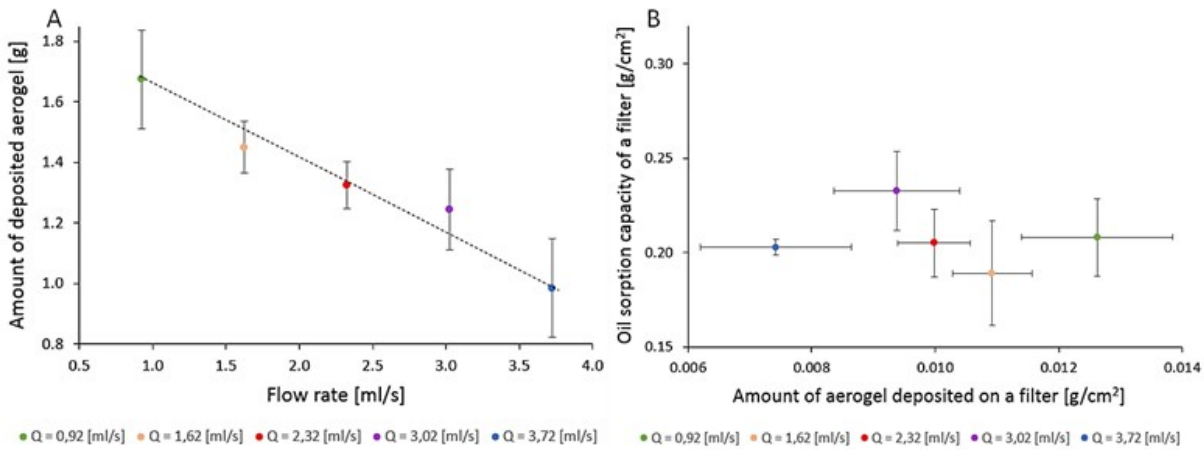

Figure 4. (A) Amount of aerogel structure deposited during one-step base modification method at various flow rates; (B) Oil sorption capacity as a function of aerogel amount deposited per filter area.

modified material's total pore volume consists of macropores – pores created by the fibres (Nowak et al., 2022b). The porous MTMS-based aerogel structure increases oil retention, so the adsorbed liquid tends neither to leak nor spread along the fibres (Nowak et al., 2023).

Another effect of increasing the flow rate is visible in SEM images, shown in Fig. 5. For two presented one-step modifications (flow rate equal to 0.92 and 2.32 mL/s), the aerogel layer takes the form of mesoporous fragments settled on the fibres. Such morphology indicates the spinodal decomposition

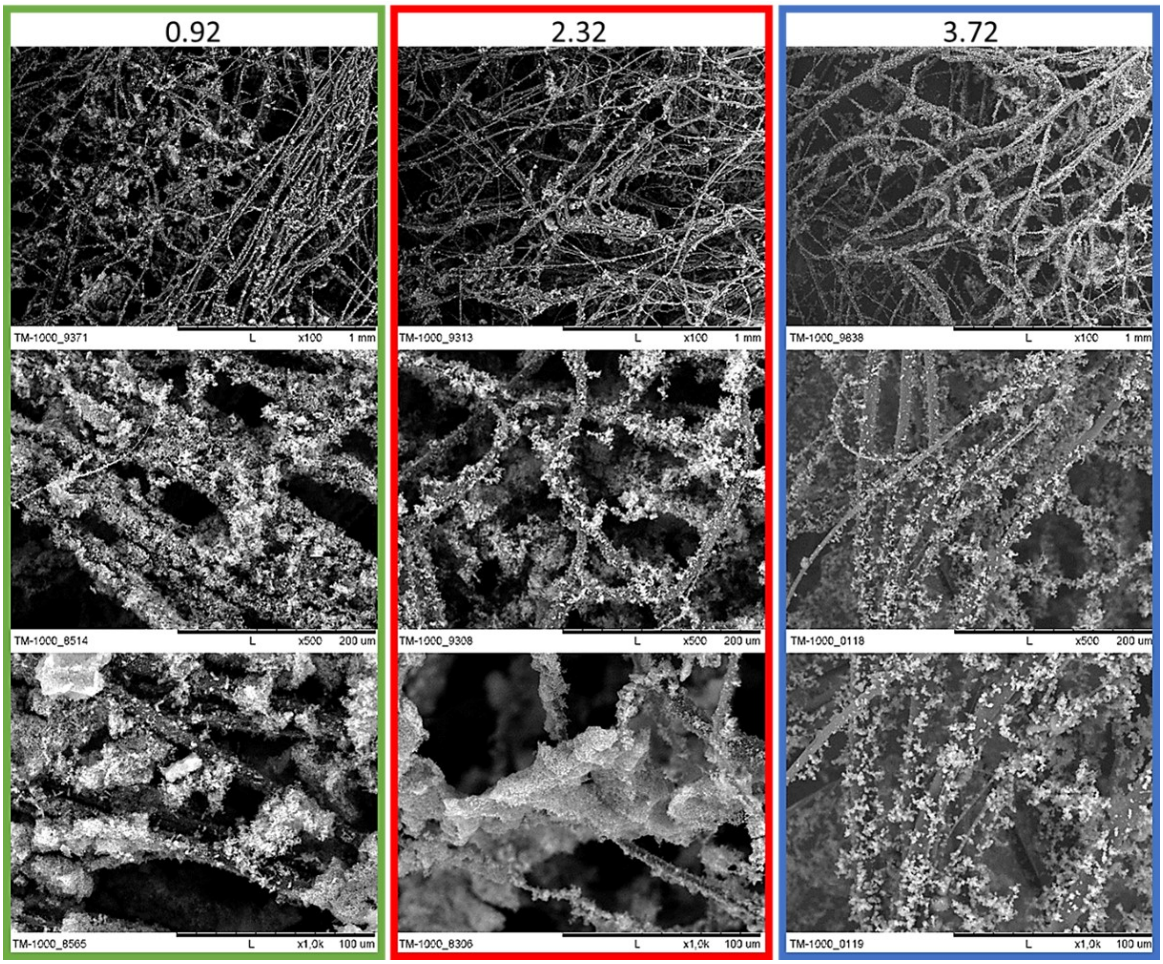

Figure 5. SEM images of filters modified with one-step base method at various flow rates (magnification 100× (top), 500× (middle) and 1000× (bottom)).

mechanism of microSCOPIC phase separation, which occurs in high pH values for precursor-rich solutions. There is more material in the places where fibres meet, which means that the condensing solution accumulates in these places due to a local increase in flow resistance. For the highest investigated flow rate (3.72 mL/s) the aerogel structure consists of small (approximately 0.2 micron) spheres. It means that the precursor concentration was lower compared to the previously described situation, or that the ammonia mixed more evenly during the second modification stage, simultaneously lowering the condensation reaction pH. Regardless of the reason for this phenomenon, the aerogel layer is more evenly distributed along the filter fibres. Fewer aerogel fragments in the fibre interconnections were observed.

SEM images show the filter internal structure, i.e. one of the middle layers. A foil layer is observed on the filter top, which is manually removed from the material. The surface foil layer formation and its influence on filter features – both sorptive properties and mist separation performance – are described in (Nowak et al., 2022b). Nonetheless, the paper shows filtration results for modified materials before and after surface layer removal (Fig. 6).

The difference between pressure drop values for filters with and without the surface layer (Fig. 6A) indicates that foil layer presence increases the airflow resistance by approximately 150-200 Pa. As indicated for the static modification method (Nowak et al., 2022a; Nowak et al., 2022b), foil removal is essential to enhance filter performance, as it is responsible for a third part of the pressure drop generated across the material. Further analysis indicates that the initial pressure drop of the modified filter is affected by the structure of the deposited aerogel. Values for materials modified with the reagent flow rates equal 0.92 and 2.32 mL/s reach 160 and 174 Pa, respectively, while for 3.72–130 Pa. Although it is still much higher than for the native filter (25 Pa), the measured pressure drop indicates that sphere-like deposits are more favourable. A more even distribution, without larger fragments (see Fig. 5) creates fewer local flow resistance spots, which translates to a smaller pressure drop overall.

The influence of both surface foil presence and aerogel deposit morphology on airflow resistance (Fig. 6A) and fractional separation efficiency is shown in Fig. 6B. Despite being the cause of a profound increase of pressure drop, the foil layer presence does not significantly affect the fractional separation efficiency, as the difference before and after foil removal equals 5–15% depending on droplet diameter. Taking into account the results for materials without a surface layer, the highest separation efficiency exhibited the sample modified with a flow rate equal to 0.92 ml/s. This sample also had the highest amount of deposited aerogel structure (Fig. 4A). A slightly lower fractional separation efficiency was noted for the sample modified with the highest reagent flow rate. Nonetheless, all samples exhibited similar separation efficiency with differences not exceeding 10%. In comparison to the native (unmodified) material, the filtration efficiency for the most penetrating particle size (MPPS) is improved fourfold, reaching 40%. Furthermore, the separation of larger droplets ($d_p \sim 1$ µm) improved from 20% to approximately 75%. The 100% efficiency is reached for smaller droplets – less than 2 micrometres for modified materials compared to 4.5 micrometres for the native filter.

The reagent flow rate influence on the amount of deposited aerogel shows the opposite tendency while applying the two-

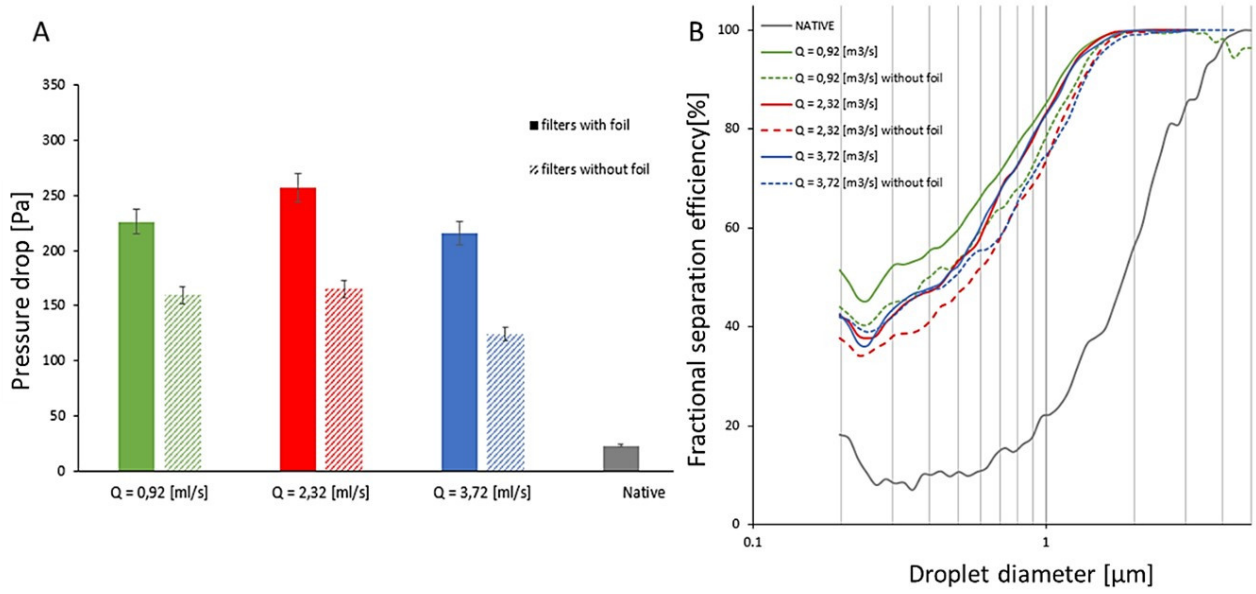

Figure 6. (A) Pressure drop and (B) oil-mist fractional separation efficiency of the native filter and filters modified with one-step base method at various flow rates with a distinction between before (solid bars and curves) and after the removal (crosshatched bars and dashed curves) of foil layer.

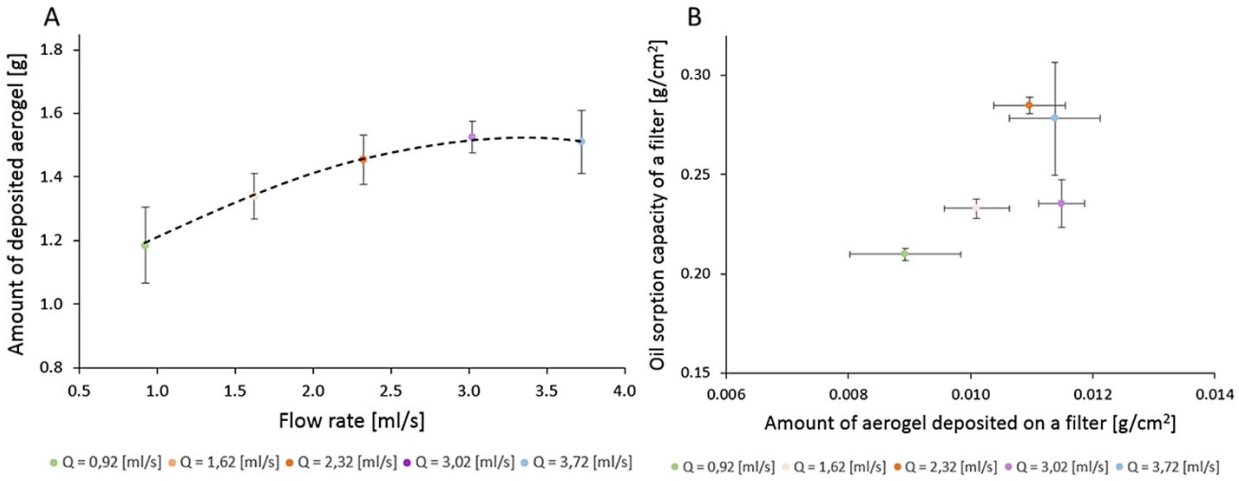

Figure 7. (A) Amount of aerogel structure deposited during two-step acid-base modification method at various flow rates; (B) Oil sorption capacity as a function of aerogel amount deposited per filter area.

step acid-base modification method (Fig. 7A) although the results for both methods are in the same order of magnitude. The aerogel structure deposition grows with the increasing reagent flow rate between 0.92 and 2.32 mL/s, flattening into a plateau at higher values. Despite slight differences in aerogel mass, their effect on sorptive properties is visible (Fig. 7B). The lowest oil sorption capacity – 0.208 g/cm^2 – exhibits the sample with the lowest aerogel amount. The oil sorption capacity increases together with the growing amount of deposited aerogel, reaching approximately 0.28 g/cm^2 for materials modified with reagent flow rates equal to 2.32 and 3.72 mL/s. The modification with a flow rate equal to 3.02 mL/s breaks the trend although the error bars for the aerogel amount results indicate that the method is not sensitive to changes in flow rate. The discrepancies between samples prepared in the same modification conditions overlap, suggesting low aerogel deposition control, but also higher adaptability of modification utilising the two-step sol-gel method.

Microscopic imagining (Fig. 8) confirms that modification utilising the two-step sol-gel method is less susceptible to changes in reagent flow rate. The aerogel structure on filter fibres looks similar to one another despite minor changes in the total deposition amount. The structure resembles a particle aggregation type, with quite uniform secondary particle size, which indicates good mixing. Local changes in pH would lead to a wide particle size distribution, which is not observed in investigated samples.

Very slight differences in the deposited structure morphology and mass translate into the modified material filtration parameters. Similarly to Fig. 6, the results of pressure drop (Fig. 9A) and fractional separation efficiency (Fig. 9B) for materials before and after removal of the top layer are presented here. Differences in the results are observed only for samples with a foil layer, for which the pressure drop ranges from 160 (for the flow of reagents equal to 0.92 mL/s) to 340 Pa (for 2.32 mL/s). The differences may result from the continuity of the foil layer – the more cracks and breaks, the lower the flow resistance generated by the surface layer. The pressure drop values coincide with the obtained fractional efficiencies of oil mist separation (Fig. 8).

Removal of the foil layer from the surface of the filters results in a decrease in the pressure drop to about 80 Pa, regardless of the flow rate of the reactants. The filtration efficiency results also do not differ significantly, reaching an efficiency of about 30% for MPPS, and complete droplet removal for sizes above 2.5 micrometres.

The comparison of the results (Fig. 10) clearly shows the predominant morphology influence of the deposited aerogel structure on the filtration parameters of the modified materials. The pressure drop (marked as dots) and overall separation efficiency (diamond marks) values do not correlate with the mass of deposited aerogel – here shown in terms of modified material packing densities. The highest pressure drop values exhibit filters modified with the one-step sol-gel method at a reagent flow rate equal to 2.32 and 3.72 mL/s – both had a distinctive aerogel morphology compared to other investigated samples (see SEM images in Fig. 5). Despite the lowest packing density, the sample modified with the one-step method with a reagent flow rate equal to 0.92 mL/s gave higher airflow resistance than samples modified with the two-step sol-gel method.

Although materials modified utilising the one-step sol-gel method exhibited higher overall separation efficiency – reaching between 48 and 55%, compared to 42-45% for the two-step method – they also caused 50-100% higher pressure drop and were more prone to morphological changes. Utilising a two-step sol-gel method allows for more even deposition and structural uniformity.

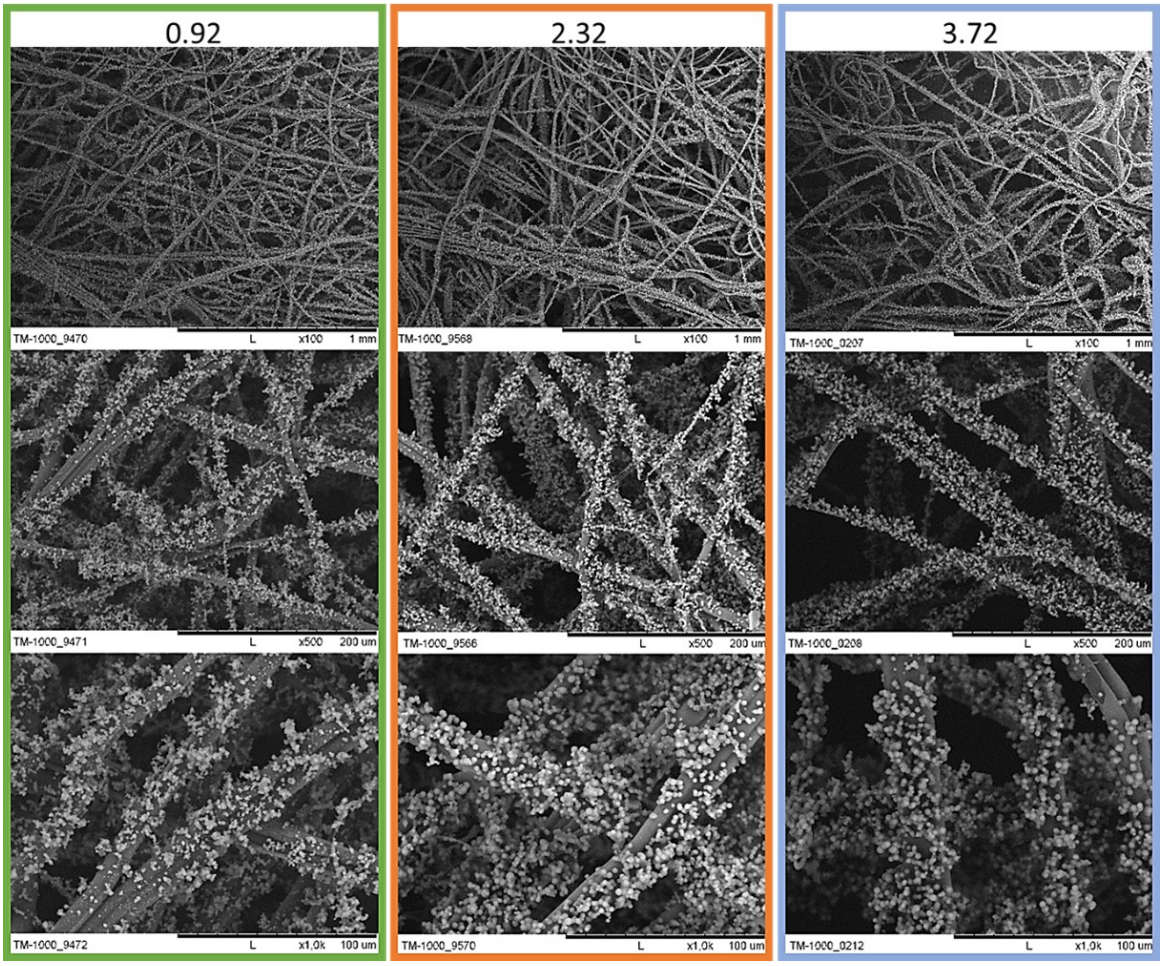

Figure 8. SEM images of filters modified with two-step acid-base method at various flow rates (magnification 100× (top), 500× (middle) and 1000× (bottom)).

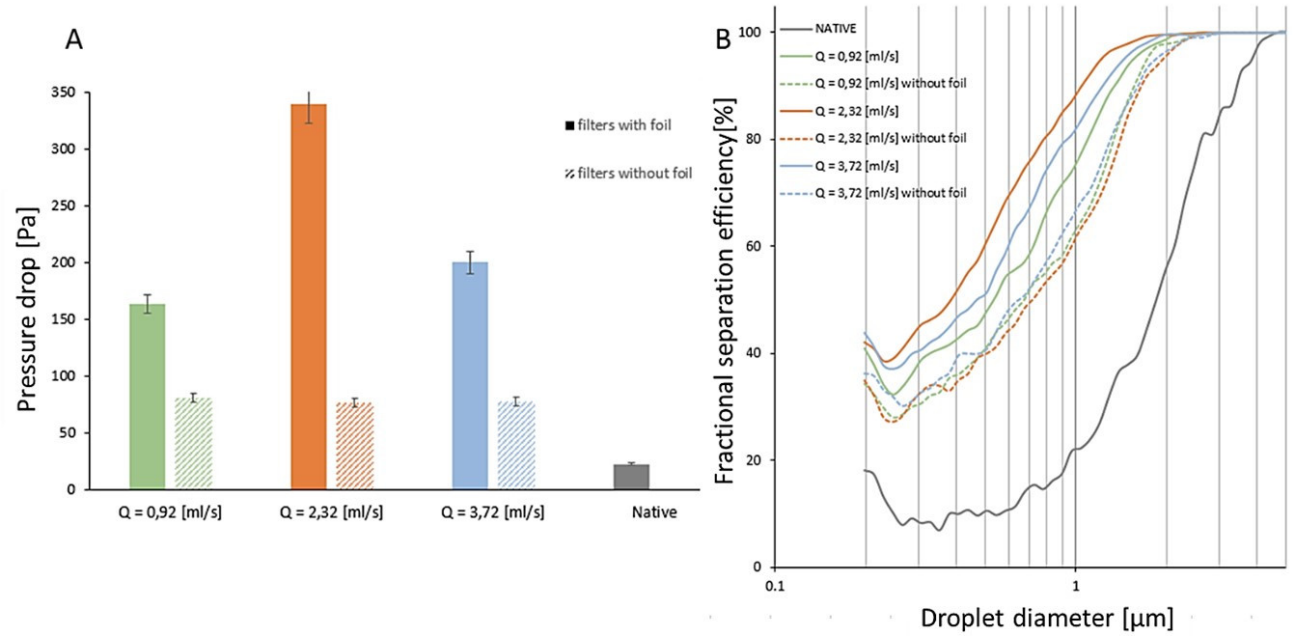

Figure 9. (A) Pressure drop and (B) oil-mist fractional separation efficiency of the native filter and filters modified with a two-step acid-base method at various flow rates with a distinction between before (solid bars and curves) and after the removal (crosshatched bars and dashes curves) of foil layer.

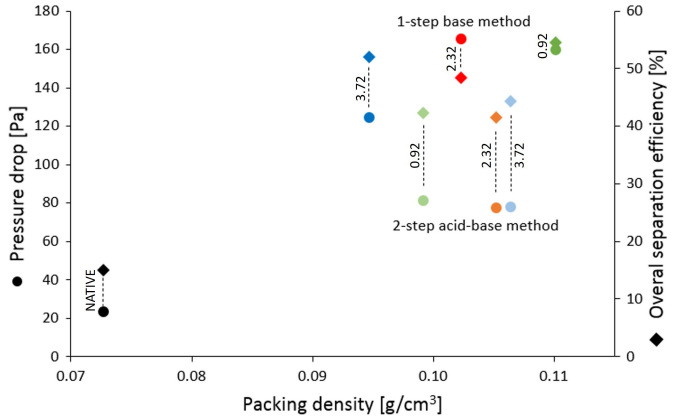

Figure 10. Pressure drop (dots) and overall separation efficiency (diamonds) of native and modified filters as a function of packing density. Numbers refer to reagent flow rate. Colours correspond with those used in Figs. 4–9.

3.2. Stage-inversion effect

Both one- and two-step methods with a reagent flow rate equal to 3.72 mL/s were chosen to investigate the stage-inversion effect. This value of flow rate was chosen because it appeared to exhibit smaller pressure drop than any others (after removing the surface foil) at a similar separation efficiency. Samples presented and described in the previous section were compiled and compared with samples where the base catalyst aqueous solution was passed through the non-woven at the first stage. The second stage consisted of a precursor and methanol solution in the one-step method or hydrolysed precursor with methanol and an aqueous solution of oxalic acid – in the two-step method. This modification method will hereinafter be referred to as the base/precursor for original samples from Section 3.1. The competitive method is to reverse the order (stage-inversion): we shall refer to it as the precursor/base method.

Fig. 11A–C shows the stage-inversion influence while the one-step sol-gel method is utilized. Passing the base catalyst as a first stage increases the deposited aerogel (Fig. 11A) – from approximately 0.8 g to 1.3 g. Mixing might be improved as the total volume of ammonia solution is lower than the second-stage precursor in methanol solution (40 mL vs 110 mL). A more uniform distribution of reagents and thus pH, or a lower degree of reagents leaching (mainly precursor) from the material volume, might explain the differences in the total amount of aerogel structure.

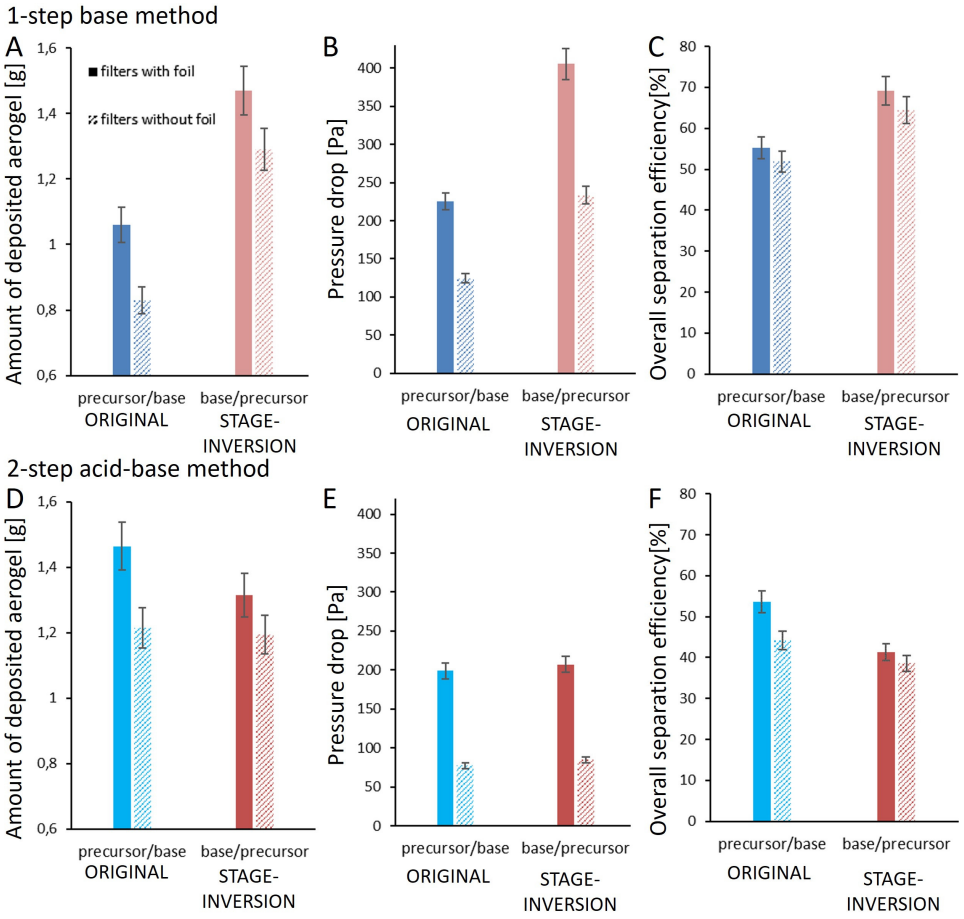

Figure 11. Influence of step-inversion on amount of deposited aerogel (A, D) pressure drop (B, E) and overall separation efficiency (C, F) of filters modified with one-step base (A–C) and two-step acid-base methods (D–F), with a distinction between before (solid bars) and after the removal (crosshatched bars) of foil layer.

Increased aerogel amount is followed by an increase in pressure drop (Fig. 11B) and overall separation efficiency (Fig. 11C) observed for the sample with the base solution used in the first stage. Similar to previously discussed samples, Fig. 11B shows a significant impact of the surface foil layer on airflow resistance. The sample base/precursor exhibits approximately 400 Pa pressure drop value before, and 240 Pa after the foil removal – which is still twice as high as for precursor/base stage order. Although stage-inversion helped to improve the overall separation efficiency (Fig. 11C), reaching 65%, the airflow resistance value cancels the usefulness of the non-woven fabric modified in this way.

Once again, the two-step sol-gel method (results in Fig. 11D–F) proved to be more stable and less susceptible to changes in the modification procedure. Both the amount of deposited aerogel structure (Fig. 11D) and pressure drop values (Fig. 11E) are within the measurement discrepancies despite the stage order. A minor decrease, of approximately 5–7%, in overall separation efficiency (Fig. 11F), is visible for the base/precursor sample.

Fractional separation efficiency results for the samples modified with the one-step (Fig. 12A) and two-step methods (Fig. 12B) show that the decrease in efficiency value by the foil layer removal does not exceed 10%. Primarily visible for droplets larger than 0.5 micrometres, up till reaching 100% efficiency for droplets of 2 (for one-step) or 3 (for two-step) micrometres in diameter. The foil layer effect on droplets close to MPPS is less significant. As explained in previous work (Nowak et al., 2022b), a surface foil layer increases separation through the interception and impaction mechanism, by increasing collector area, simultaneously decreasing the efficiency for droplets separated via diffusion mechanism – presumably by locally accelerating the airflow. At the MPPS value, both effects on described mechanisms cancel each other out, hence similar values are obtained for filters with and without the foil layer.

SEM images (Fig. 13) show a great aerogel morphology variation, which explains the filtration performance differences of non-wovens modified with the one-step method. As previously assumed, a higher volume of precursor solution passing through the material during the modification second stage leads to better mixing with the condensation catalyst and a higher residence time of reacting solution in material volume. SEM images of the base/precursor sample show a microporous, dendrite-like aerogel structure growing towards the space between the fibres rather than along them. Such a deposition of the aerogel structure leads to a significant increase in the effective surface of the fibre, which leads to an increase in separation efficiency, but at the same time, it poses a large resistance to the flowing air (see Figs. 11B–C).

Still observable, though definitely not as significant dendrite-like structure growth is visible for the sample base/precursor modified with the two-step sol-gel method (Fig. 13). Aerogel secondary particles tend to grow away from the fibre surface, creating a less uniform structure with a wider particle size distribution than a "single-particle" layer observed for precursor/base two-step modification. Although this difference is marginal, it might explain the slight difference in fractional

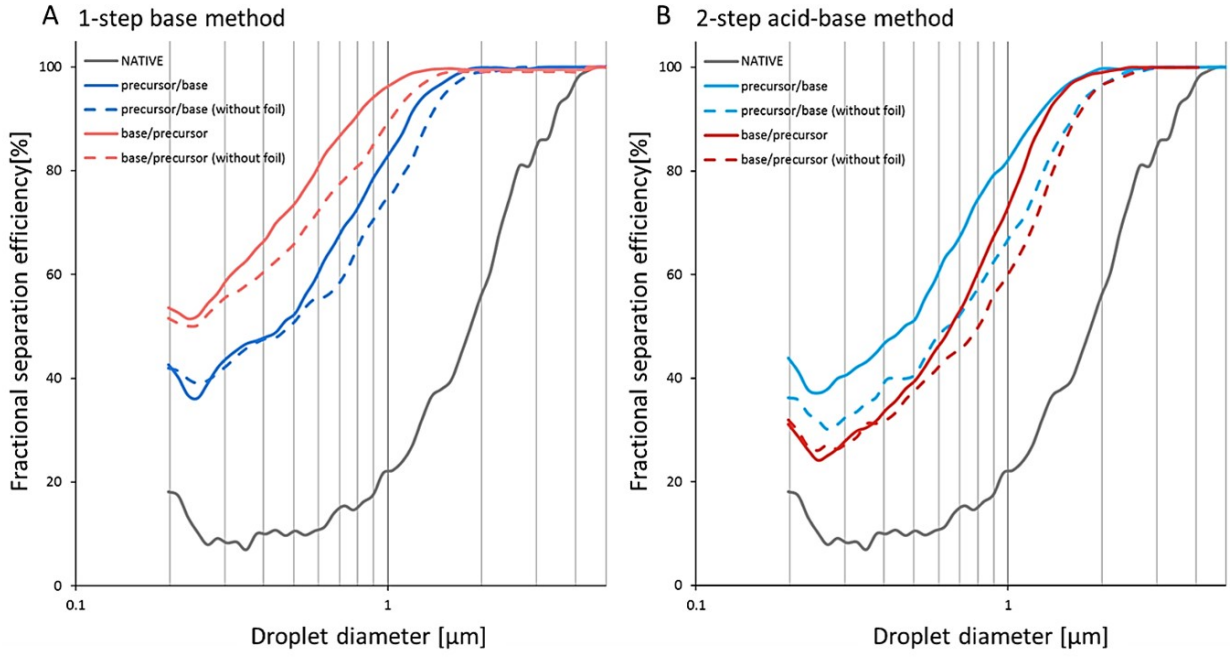

Figure 12. Influence of step-inversion on fractional separation efficiency for filters modified with one-step base (A) and two-step acid-base methods (B), with a distinction between before (solid curves) and after the removal (dashes curves) of the foil layer.

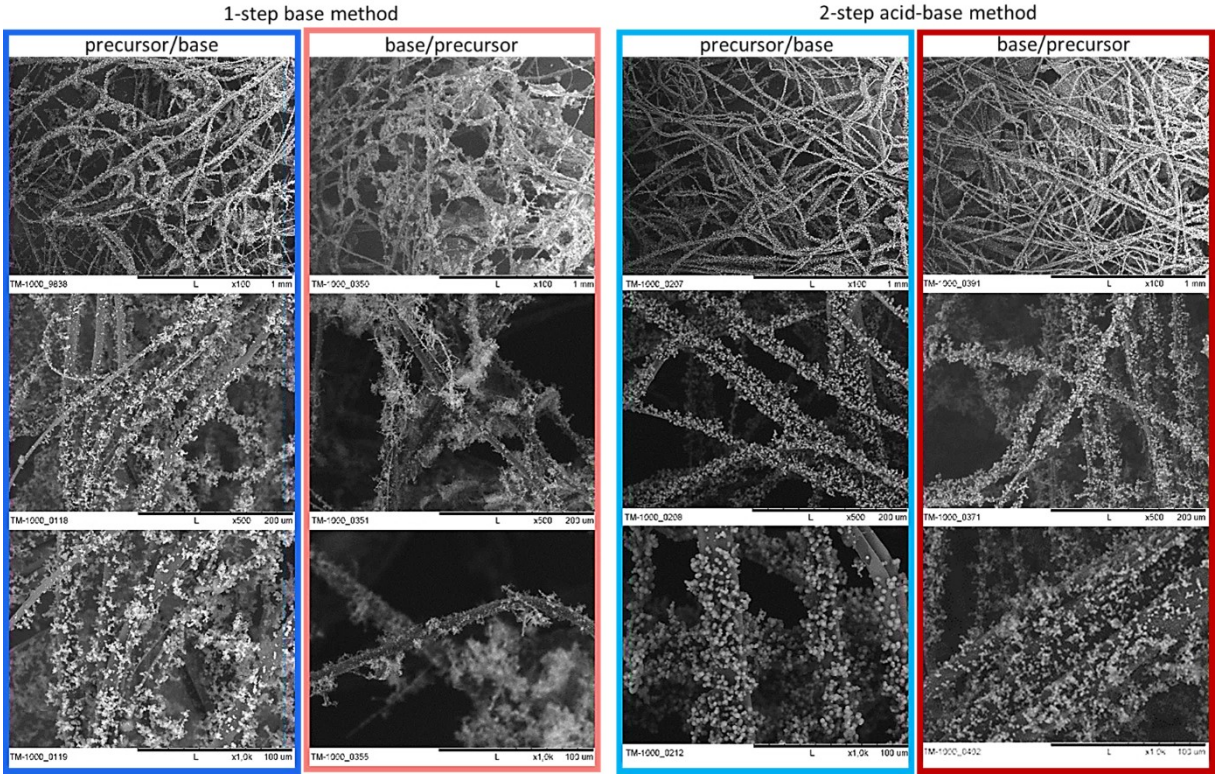

Figure 13. SEM images of filters modified with one-step base and two-step acid-base methods with inversed modification steps (magnification 100× (top), 500× (middle) and 1000× (bottom)).

separation efficiency, as seen in Fig. 12.

Due to the impact of the modification on the separation efficiency and pressure drop, both positive and negative influences should be taken into account to compare and select the best process conditions. For this purpose, the filter Quality Factor (QF) was introduced (Brown, 1993), which is calculated from Equation (3):

$$QF = -\ln\frac{(1-E)}{\Delta P} \tag{3}$$

where: E – separation efficiency [%] and ΔP – pressure drop across the filter [Pa].

The Quality Factor may be calculated for overall filtration efficiency total or individual droplet diameters (Fig. 14). This paper shows the QF for overall filtration efficiency and droplet fractions of 1 μm and 0.3 μm in diameter. The first one is a typical value present in filter design assumptions, while the latter corresponds to the drops most strongly penetrating the filter structure.

Despite moderate enhancement of filtration efficiency, the filter modified with the two-step sol-gel method with the stage order precursor/base exhibits the highest QF values. This is due to balancing the increase in separation efficiency with the negative impact of the aerogel structure deposition on the increase in airflow resistance. The most glaring example of which is the one-step base/precursor sample. Despite the distinctly highest separation efficiency, the pressure drop of almost 250 Pa overshadows the positive modification impact.

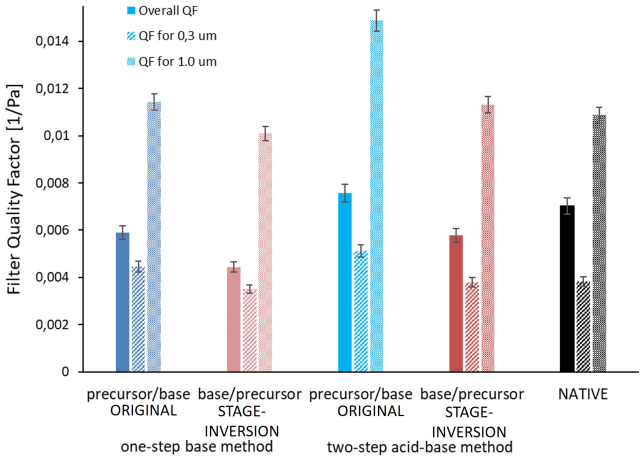

Figure 14. Quality Factor for droplet diameter equal to 0.3 μm, 1.0 μm and overall separation efficiency for filters: native and modified with one- and two-step sol-gel methods with stage inversion and reagent flow rate equal to 3.72 mL/s.

4. DISCUSSION

Among the proposed methods of aerogel synthesis, adapted to modify non-woven filters, the two-stage sol-gel method showed not only a better improvement of separation properties but also greater adaptability. The modification based on the single-step synthesis showed a high susceptibility to changes in the process conditions, which resulted in lower repeatability and inhomogeneity of the deposited structure.

Since we have demonstrated the possibility of fibre modification with sol-gel techniques using the flow method, it is worth briefly discussing the possibilities of increasing the scale of the process. The proposed layout with the modification cell in which the material is placed is treated as a semi-step before scaling. However, it seems natural to be able to increase the scale by numbering-up – i.e. connecting many cells in parallel (Patience and Boffito, 2020). The system could be powered by a single pump and have one set of inlet and outlet tanks. Such a solution may be interesting from an economic point of view (Weber and Snowden-Swan, 2019). Interconnection through numbering-up offers great flexibility due to the possibility of adapting some of the system's cells to run parallel modifications in different conditions. However, due to the time needed to install and replace the modified filter materials and their transfer for APD, such a system cannot operate continuously. In addition, the size of the material is limited by the size of the modifying cell used.

The most popular continuous production system is roll-to-roll. Due to the modularity of production, it is possible to use many types of coatings (Søndergaard et al., 2013). Thus, it is possible to functionalize (Rao et al., 2018) and modify the surface of non-woven materials (Cheng and Gupta, 2018), including those produced with electrospinning (Xu et al., 2016). Recently continuous manufacturing of aerogel-impregnated blankets on a roll-to-roll system is under development in Aerogel Technologies and DLR. Although transfer from the currently described modification in flow-cell would require optimisation de novo, all vital stages can be achieved in separate modules. The system would consist of an unwinder, three separate reagent baths (one for IPA prewetting and two for main modification stages), possibly separated by a squeezing roll, evaporating/drying module (for example a hot-air dryer) and a rewinder (Fig. 15). Despite being the most common practice for continuous production, the roll-to-roll system would entail large investment costs.

5. CONCLUSIONS

In the article, we presented a method of modifying filters by depositing aerogel on their fibre surface in the flow process. This approach aligns with the spirit of chemical engineering, as it enables better control of the process and more efficient use of raw materials (reactants) and scalability. Of the two methods discussed – one-step, alkaline and two-step, acid-base – the latter exhibits a more uniform, built of same-size secondary particle aerogel structure layer. Thus, this structure seems more suitable for oil-mist filtration, as it does not cause high airflow resistance.

Other important issues of the flow modification process (which have not appeared during the batch process described in our previous works) were the influence of reagent flow rate and sequence of reactant flow stages (base applied before precursor flow or vice versa). During the one-step method the influence of reagent flow rate on oil sorption capacity, pressure drop and filtration efficiency was rather weak, while in the case of the two-step process, the higher flow rate led in general to higher sorption capacity, which resulted in higher filtration efficiency. If the two-stage method is chosen (which, as mentioned above, is more advantageous), the highest possible flow rate of modifying solutions should be used. Of course, our studies only included flow rates up to 3.72 mL/s. It should be expected that absurdly high intensity, often exceeding this value, will not cause a further improvement of the filter properties and perhaps even their deterioration.

Regarding the sequence of reactant flow stages, the precursor/base process gives better results than the base/precursor, characterized by a higher quality factor. In the case of one-step synthesis, it manifests itself in a smaller pressure drop

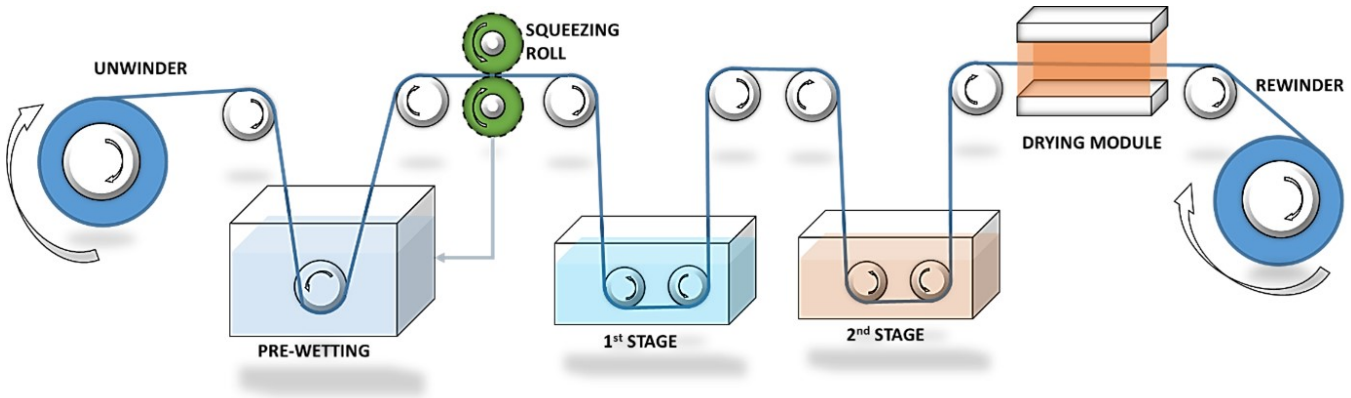

Figure 15. Schematic proposition of roll-to-roll modification system.

value, while the two-step method results in higher overall separation efficiency. It is worth noting that the modification in the precursor/base configuration leads to an increase of the quality factor of the filter (relative to the native filter). This increase is observed both in total efficiency and in the efficiency of the most penetrating particles or particles with a size of 1 micron. Although significantly higher quality factor values are observed for two-stage modification, these values are also higher in the case of one-stage modification than those of the native filter.

ACKNOWLEDGMENTS

This work was supported by The National Centre for Research and Development, Poland – project "Oil removal from gas and liquid streams thanks to filter media modified by aerogel" LIDER/011/L-6/14/NCBR/2015. The authors would like to thank Prof. Andrzej Krasiński and Dr Łukasz Werner for their help in creating a cell for flow-system modification.

SYMBOLS

ρ_P	DEHS oil density, g/cm^3
d_p	droplet size, μm
E	separation efficiency, %
m_{ag}	the mass of deposited aerogel, g
m_{PP}	mass of polypropylene filter, g
QF	filter quality factor, 1/Pa
u_0	linear gas velocity, m/s
V	material volume, cm^3
α	packing density, %
ΔP	pressure drop across the filter, Pa
ρ_{PP}	polypropylene density, g/cm^3
ρ_{sk}	MTMS skeletal density, g/cm^3

REFERENCES

Agranovski I.E., Braddock R.D., 1998. Filtration of liquid aerosols on wettable fibrous filters. *AIChE J.*, 44, 2775–2783. DOI: 10.1002/aic.690441218.

Azani A., Halin D.C., Razak K.A., Abdullah M.M.A.B., Salleh M.A.A.M., Mahmed N., Ramli M.M., Azhari A.W., Chobpattana V., 2019. Recent graphene oxide/TiO_2 thin film based on self-cleaning application. *IOP Conf. Ser.: Mater. Sci. Eng.*, 572, 012079. DOI: 10.1088/1757-899X/572/1/012079.

Borzęcka N.H., Nowak B., Gac J.M., Głaz T., Bojarska M., 2020. Kinetics of MTMS-based aerogel formation by the sol-gel method-experimental results and theoretical description. *J. Non-Cryst. Solids*, 547, 120310. DOI: 10.1016/j.jnoncrysol.2020.120310.

Borzęcka N.H., Nowak B., Pakuła R., Przewodzki R., Gac J.M., 2023. Diffusion/reaction limited aggregation approach for microstructure evolution and condensation kinetics during synthesis of silica-based alcogels. *Int. J. Mol. Sci.*, 24, 1999. DOI: 10.3390/ijms24031999.

Brinker C.J., Keefer K.D., Schaefer D.W., Ashley C.S., 1982. Sol-gel transition in simple silicates. *J. Non-Cryst. Solids*, 48, 47-64. DOI: 10.1016/0022-3093(82)90245-9.

Brown R.C., 1993. Electrically charged filter material. In: *Air filtration: An integrated approach to the theory and applications of fibrous filters*. Pergamon Press, New York, 121.

Charvet A., Gonthier Y., Gonze E., Bernis A., 2010. Experimental and modelled efficiencies during the filtration of a liquid aerosol with a fibrous medium. *Chem. Eng. Sci.*, 65, 1875–1886. DOI: 10.1016/j.ces.2009.11.037.

Cheng C., Gupta M., 2018. Roll-to-roll surface modification of cellulose paper via initiated chemical vapor deposition. *Ind. Eng. Chem. Res.*, 57, 11675-11680. DOI: 10.1021/acs.iecr.8b03030.

Dong H., Brook M.A., Brennan J.D., 2005. A new route to monolithic methylsilsesquioxanes: gelation behavior of methyltrimethoxysilane and morphology of resulting methylsilsesquioxanes under one-step and two-step processing. *Chem. Mater.*, 17, 2807–2816. DOI: 10.1021/cm050271e.

Gac J.M., 2015. A simple numerical model of pressure drop dynamics during the filtration of liquid aerosols on fibrous filters. *Sep. Sci. Technol.*, 50, 2015–2022. DOI: 10.1080/01496395.2015.1014496.

Haq E.U., Zaidi S.F.A., Zubair M., Karim M.R.A., Padmanabhan S.K., Licciulli A., 2017. Hydrophobic silica aerogel glass-fibre composite with higher strength and thermal insulation based on methyltrimethoxysilane (MTMS) precursor. *Energy Build.*, 151, 494–500. DOI: 10.1016/j.enbuild.2017.07.003.

Hüsing N., Schubert U., 1998. Aerogels–airy materials: chemistry, structure, and properties. *Angew. Chem. Int. Ed.*, 37, 22–45. DOI: 10.1002/(SICI)1521-3773(19980202)37:1/2<22::AID-ANIE22>3.0.CO;2-I.

Ismail W. N. W., 2016. Sol–gel technology for innovative fabric finishing – a review. *J. Sol-Gel Sci. Technol.*, 78, 698–707. DOI: 10.1007/s10971-016-4027-y.

Jackiewicz A., Werner Ł., 2015. Separation of nanoparticles from air using melt-blown filtering media. *Aerosol Air Qual. Res.*, 15, 2422–2435. DOI: 10.4209/aaqr.2015.04.0236.

Joung Y.C., Park J.C., Kim M.W., 2018. *System for injecting functional solution for fabric and method for manufacturing fabric using same*. U.S. Patent No. US9951450B2.

Kampa D., Wurster S., Buzengeiger J., Meyer J., Kasper G., 2014. Pressure drop and liquid transport through coalescence filter media used for oil mist filtration. *Int. J. Multiph. Flow*, 58, 313–324. DOI: 10.1016/j.ijmultiphaseflow.2013.10.007.

Kampa D., Wurster S., Meyer J., Kasper G., 2015. Validation of a new phenomenological "jump-and-channel" model for the wet pressure drop of oil mist filters. *Chem. Eng. Sci.*, 122, 150–160. DOI: 10.1016/j.ces.2014.09.021.

Kim C.Y., Lee J.K., Kim B.I., 2008. Synthesis and pore analysis of aerogel-glass fiber composites by ambient drying method. *Colloids Surf. A*, 313–314, 179–182. DOI: 10.1016/j.colsurfa.2007.04.090.

Kim S.J., Chase G., Jana S.C., 2016. The role of mesopores in achieving high efficiency airborne nanoparticle filtration using aerogel monoliths. *Sep. Purif. Technol.*, 166, 48–54. DOI:

10.1016/j.seppur.2016.04.017.

Kolb H.E., Watzek A.K., Zaghini Francesconi V., Meyer J., Dittler A., Kasper G., 2018. A mesoscale model for the relationship between efficiency and internal liquid distribution of droplet mist filters. *J. Aerosol Sci.*, 123, 219–230. DOI: 10.1016/j.jaerosci.2018.05.013.

Liew T.P., Conder J.R., 1985. Fine mist filtration by wet filters – I. Liquid saturation and flow resistance of fibrous filters. *J. Aerosol Sci.*, 16, 497–509. DOI: 10.1016/0021-8502(85)90002-3.

Linhares T., de Amorim M.T.P., Durães L., 2019. Silica aerogel composites with embedded fibres: a review on their preparation, properties and applications. *J. Mater. Chem. A*, 7, 22768–22802. DOI: 10.1039/C9TA04811A.

Mazrouei-Sebdani Z., Naeimirad M., Peterek S., Begum H., Galmarini S., Pursche F., Malfait W.J., 2022. Multiple assembly strategies for silica aerogel-fiber combinations – A review. *Mater. Des.*, 223, 111228. DOI: 10.1016/j.matdes.2022.111228.

Mekonnen B.T., Ding W., Liu H., Guo S., Pang X., Ding Z., Seid M.H., 2021. Preparation of aerogel and its application progress in coatings: A mini overview. *J. Leather Sci. Eng.*, 3, 25. DOI: 10.1186/s42825-021-00067-y.

Mosanenzadeh S.G., Saadatnia Z., Karamikamkar S., Park C.B., Naguib H.E., 2020. Polyimide aerogels with novel bimodal micro and nano porous structure assembly for airborne nano filtering applications. *RSC Adv.*, 10, 22909–22920. DOI: 10.1039/D0RA03907A.

Mullins B.J., Agranovski I.E., Braddock R.D., Ho C.M., 2004. Effect of fiber orientation on fiber wetting processes. *J. Colloid Interface Sci.*, 269, 449–458. DOI: 10.1016/S0021-9797(03)00729-X.

Nowak B., Bonora M., Gac J.M., 2022a. Modification of polypropylene fibrous filters with MTMS-based aerogel for improvement of oil mist separation properties – Experimental and theoretical study. *J. Environ. Chem. Eng.*, 10, 107852. DOI: 10.1016/j.jece.2022.107852.

Nowak B., Bonora M., Winnik M., Gac J.M., 2023. An effect of fibrous filters modification with MTMS aerogel structure on oil mist filtration dynamics. *J. Aerosol Sci.*, 170, 106147. DOI: 10.1016/j.jaerosci.2023.106147.

Nowak B., Bonora M., Zuzga M., Werner Ł., Jackiewicz-Zagórska A., Gac J.M., 2022b. MTMS-based aerogel structure deposition on polypropylene fibrous filter – Surface layer effect and distribution control for improvement of oil aerosol separation properties. *J. Environ. Chem. Eng.*, 10, 108410. DOI: 10.1016/j.jece.2022.108410.

Nowak B., Gac J.M., Bojarska M., Jackiewicz A., Werner Ł., 2017. Modification of filtering materials with aerogel for improvement of oil mist separation. *Inż. Ap. Chem.*, 1, 17–20.

Nowak B., Kawka M., Wierzchowski K., Sykłowska-Baranek K., Pilarek M., 2021. MTMS-based aerogel constructs for immobilization of plant hairy roots: Effects on proliferation of *Rindera graeca* biomass and extracellular secretion of naphthoquinones. *J. Funct. Biomater.*, 12, 19. DOI: 10.3390/jfb12010019.

Ortelli S., Costa A.L., Dondi M., 2015. TiO_2 nanosols applied directly on textiles using different purification treatments. *Materials*, 8, 7988-7996. DOI: 10.3390/ma8115437.

Patience G.S., Boffito D.C., 2020. Distributed production: Scale-up vs experience. *Adv. Manuf. Process.*, 2, e10039. DOI: 10.1002/amp2.10039.

Penner T., Meyer J., Dittler A., 2021. Oleophilic and oleophobic media combinations – Influence on oil mist filter operating performance. *Sep. Purif. Technol.*, 261, 118255. DOI: 10.1016/j.seppur.2020.118255.

Rao E., McVerry B., Borenstein A., Anderson M., Jordan R.S., Kaner R.B. 2018. Roll-to-roll functionalization of polyolefin separators for high-performance lithium-ion batteries. *ACS Appl. Energy Mater.*, 1, 3292–3300. DOI: 10.1021/acsaem.8b00502.

Shams-Ghahfarokhi F., Khoddami A., Mazrouei-Sebdani Z., Rahmatinejad J., Mohammadi H., 2019. A new technique to prepare a hydrophobic and thermal insulating polyester woven fabric using electro-spraying of nano-porous silica powder. *Surf. Coat. Technol.*, 366, 97–105. DOI: 10.1016/j.surfcoat.2019.03.025.

Søndergaard R.R., Hösel M., Krebs F.C., 2013. Roll-to-roll fabrication of large area functional organic materials. *J. Polym. Sci., Part B: Polym. Phys.*, 51, 16-34. DOI: 10.1002/polb.23192.

Starnoni M., Manes C., 2022. On the interplay between pressure and gravitational forces in coalescing filters. *J. Aerosol Sci.*, 162, 105953. DOI: 10.1016/j.jaerosci.2022.105953.

Sun W., Chen D.R., 2002. Filter loading characteristics of liquid-coated particles. *IAQ Filtration Conference, American Filtration and Separation (AFS) Society*, Cincinnati, Ohio, USA.

Tepekiran B.N., Calisir M.D., Polat Y., Akgul Y., Kilic A., 2019. Centrifugally spun silica (SiO_2) nanofibers for high-temperature air filtration. *Aerosol Sci. Technol.*, 53, 921–932. DOI: 10.1080/02786826.2019.1613514.

Weber R.S., Snowden-Swan L.J., 2019. The economics of numbering up a chemical process enterprise. *J. Adv. Manuf. Process.*, 1, e10011. DOI: 10.1002/amp2.10011.

Wu H., Chen Y., Chen Q., Ding Y., Zhou X., Gao H., 2013. Synthesis of flexible aerogel composites reinforced with electrospun nanofibers and microparticles for thermal insulation. *J. Nanomater.*, 2013, 375093. DOI: 10.1155/2013/375093.

Xu C., Yu Y., Si X., 2021. Oil-mists coalescence performance of fibrous filters with superoleophilic and superoleophobic surface. *Chem. Eng. Res. Des.*, 172, 235–241. DOI: 10.1016/j.cherd.2021.06.013.

Xu J., Liu C., Hsu P.-C., Liu K., Zhang R., Liu Y., Cui, Y., 2016. Roll-to-roll transfer of electrospun nanofiber film for high-efficiency transparent air filter. *Nano Lett.*, 16, 1270–1275. DOI: 10.1021/acs.nanolett.5b04596.

Yarin A.L., Chase G.G., Liu W., Doiphode S.V., Reneker D.H., 2006. Liquid drop growth on a fibre. *AIChE J.*, 52, 217–227. DOI: 10.1002/aic.10661.